
Verification of ESOC Ionosphere Modeling and Status of IGS Intercomparison Activity

J. Feltens¹, J.M. Dow², T.J. Martín-Mur², C. García Martínez³, M.A. Bayona-Pérez³

1. EDS at Orbit Attitude Division, ESA, European Space Operations Centre, Robert-Bosch-Str. 5, D-64293 Darmstadt, Germany

2. ESOC

3. GMV at ESOC

Abstract

ESOC is planning to extend the use of IGS data also for ionospheric modeling. It is intended to provide ionospheric VTEC models and receiver/satellite differential delay values as new IGS products - besides orbits, earth orientation parameters and station coordinates. Different mathematical models were worked out to represent the ionosphere as single layer. ESOC-internally a short term analysis of these models indicated reliable performance.

In preparation of the IGS workshop in Silver Spring a comparison of ionosphere VTEC models originating from different Analysis Centers was organized. This comparison offers the opportunity to verify the modeling & implementations of the participating AC's.

ESOC will use the knowledge earned from this comparison, to define its final mathematical modeling and implement it in the Ionosphere Monitoring Facility (IONMON), which is under development at ESOC. Apart from the routine provision of ionospheric products to IGS, it is intended to use the ionosphere models for the support of other ESA-missions, e.g. ERS and ENVISAT.

1 INTRODUCTION

Since June 1992 ESOC participates as an Analysis Center at IGS. ESOC's activities within IGS include the routine provision of rapid and precise GPS orbits, earth orientation parameters, GPS satellite and station clock parameters, and ground station coordinates (SINEX), as well as GPS data tracking and retrieval from own ESOC tracking sites (currently, March 1996, these are: Kiruna, Kourou, Malindi, Maspalomas, Perth and Villafranca) on routine basis.

The transmission of navigation signals on two well defined frequencies is one of the basic characteristics of GPS. On the other hand, ionospheric effects, that are acting on satellite transmitted signals, are frequency-dependent. So, more or less as a by-product, the global dual-frequency GPS data, daily retrieved as part of ESOC's IGS activities, offer the opportunity to perform some kind of ionosphere monitoring to update ionosphere models using actual GPS data, and to provide these updated ionosphere models for other ESA missions to allow them to make ionospheric corrections on their own tracking data. This was the basic idea to concept and to establish an Ionosphere Monitoring Facility (IONMON) at ESOC.

The IONMON is currently under development, and a prototyping version is close to be operational. This prototyping version was used for an intercomparison of ionosphere products between ESOC and other Analysis Centers in preparation of the IGS workshop in Silver Spring in March 1996 (see also next chapter). The results of this comparison were used to verify the performance of mathemat-

ical modeling in ESOC fits to TEC data. Once the final IONMON software is established, it will replace the prototyping version.

2 IONOSPHERE MODELS - A NEW PRODUCT OF IGS ?

The opportunity to exploit dual-frequency GPS data from IGS for ionosphere monitoring was also recognized by other members of the IGS, and following the IGS workshop in Potsdam in May 1995 it was suggested that a comparison of ionospheric products should be organized between the Analysis Centers.

Several of the Analysis Centers participating in the IGS (JPL, EMR, CODE), as well as some external processing centers (DLR Neustrelitz, University of New Brunswick (UNB) - these will in the following text be denoted as Analysis Centers too) have already experience with the evaluation of ionospheric parameters from dual-frequency GPS data and possess dedicated software. Others (ESOC) are currently implementing ionospheric modeling into their software, as was already mentioned in the above chapter.

In order to bring all the varying activities into one common direction of a routine provision of ionospheric information as a new product of the IGS, an intercomparison of ionosphere products originating from the different Analysis Centers was organized in preparation of the IGS workshop in Silver Spring in March 1996. The intent of this intercomparison was to find out:

- How ionosphere modeling is done at the different Analysis Centers, i.e. which mathematical models, which update rate, which geographical extent, etc.
- Which accuracies are currently obtained.

It is the intent of this paper to present the results of ESOC mathematical model verification in special (see above chapter) and to summarize the intercomparison between the different Analysis Centers in general.

3 MATHEMATICAL MODELS USED AT ESOC

Generally the IONMON offers so called single layer models to represent ionospheric VTEC, i.e. TEC observations are modeled as follows:

$$l + \varepsilon = Map \cdot VTEC + k_j + k^i \quad (3.1)$$

where:

l	TEC observable,
ε	observation noise,
Map	mapping function projecting the observed TEC to the vertical,
$VTEC$	single layer model to represent the vertical TEC,

k_j	receiver differential delay,
k^i	satellite differential delay.

The following general assumptions are made:

- Assumed height of ionospheric shell: $h_I = 350 \text{ km}$.
- Mapping function: Either standard (see e.g. Mannucci et al, 1993), or the so called Q -factor mapping function (see Newby, 1992).
- Elevation cutoff is set equal to $el_{min} = 20^\circ$.
- Elevation-dependent weights are applied to favour high-elevation TEC observables and to prejudice low-elevation TEC observables:

$$W = e^{-\alpha(1 - el/90^\circ)^\beta} \quad \text{with} \quad el = \text{elevation}, \alpha = \beta = 2$$

- The reference frame used is aligned to the Sun's direction and to the geomagnetic pole. The algorithm of Biel (1990) is applied to transform from the geographic frame into the geomagnetic one.
- Fits of ionosphere models to TEC observation data are done in batch estimation mode.

Initially restricted to the above listed simple modeling, it is planned to extend the IONMON in successive versions for parameter updates in sequential estimation mode as well as to include more sophisticated models to represent the ionosphere's electron content, e.g. profiles and other physically based models, and evaluation of non-GPS and of satellite-to-satellite tracking data.

Depending on geographic extent, ESOC mathematical modeling can be classified into polynomial, spherical harmonic and Gauss-function fits, as described in the following sections.

3.1 Polynomials for Local VTEC representations

Polynomials (ref. R5) are fitted to TEC data which were collected at a certain ESA ground site to obtain a local VTEC model around that ground site in form of a higher-order surface. Fits are done in 6-hour time intervals, and the satellite/receiver differential delay values are constrained to 0.5 nanoseconds with respect to the values obtained from the nighttime fit (see Section 3.4). Polynomial development is linear in latitude and quadratic in local time (cubic for the equatorial ESA stations Kourou and Malindi).

3.2 Spherical Harmonics for Global/Regional VTEC Models

Degree and order $n, m = 8$ spherical harmonics (ref. R5) are fitted to regionally (e.g. Europe) and globally collected TEC data. The coefficients a_{10} , a_{11} and b_{11} , which define the origin of the coordinate reference, are kept fixed with zero. Fits are done in 12-hour time intervals, and the satellite/receiver differential delay values are constrained to 0.5 nanoseconds with respect to the values obtained from the nighttime fit (see Section 3.4).

3.3 Gauss-Type Exponential Functions for Global VTEC Models

The method to model the global VTEC with Gauss-Type Exponential (GE) functions was worked out at ESOC, and is under testing now. It is out of the scope of this paper to present the GE-function theory, so only the very basic can be shown here: The VTEC of the above Equation (3.1) is represented by a GE-function single layer model as follows:

$$\begin{aligned}
 VTEC = \Xi + G \cdot e^{-a_1x - a_2x^2 - a_3x^3 - \dots - a_{2n}x^{2n}} \\
 \cdot e^{-b_1y - b_2y^2 - b_3y^3 - \dots - b_{2m}y^{2m}} \\
 \cdot e^{-c_1xy - c_2x^2y - c_3xy^2 - \dots - c_{l-k+2}x^{k-1}y - \dots - c_lxy^{k-1}}
 \end{aligned} \tag{3.2}$$

with

$$k = \text{minimum}(2n, 2m) \quad l = k \cdot (k - 1) / 2$$

where:

<i>VTEC</i>	single layer VTEC, now represented by a GE-function,
<i>x</i>	independent variable; <i>x</i> is a function of local time,
<i>y</i>	independent variable; <i>y</i> is a function of latitude,
Ξ	constant offset,
<i>G</i>	amplitude,
<i>a_i</i>	<i>x</i> -coefficients,
<i>b_j</i>	<i>y</i> -coefficients,
<i>c_q</i>	mixed terms coefficients.

The constant offset Ξ , the amplitude *G* and the coefficients *a_i*, *b_j*, *c_q* are estimated as unknowns. The degree and order of GE-function development must always be an even one - therefore **2n** and **2m** in the above Equation (3.2). The number of mixed terms depends on the degree and order of development. If *k* is the lower one of degree and order, the total number of mixed terms is given by $l = k \cdot (k-1) / 2$. Local time and geomagnetic latitude are re-scaled into the *x, y* variables to get appropriate arguments for the GE-function. Unlike polynomials and spherical harmonics, GE-functions are not linear in their coefficients, i.e. initial values are required to establish linear observation equations. This problem can be overcome, when the GE-function is logarithmerized. Provided initial values for the constant offset Ξ and for the satellite/receiver differential delays are known, the observation equation (3.1) can be set up in logarithmerized form, and a first iteration is made in logarithmic mode to get initial values for the amplitude *G* and the coefficients *a_i*, *b_j*, *c_q*. All successive iterations are then made in normal mode with linearized observation equations.

Ref. R6 presents the detailed description of the GE-function algorithm development from the first idea to the final formulae (i.e. detailed mathematics, partials, scaling of *x, y*, first iteration in logarithmic mode, etc.).

Global TEC data are fitted to GE-functions in 12-hour intervals. Degree of development, i.e. local time component, is **2n = 10** and order, i.e. latitude component, is **2m = 6**. Including the constant offset, the amplitude and the mixed terms, a total of 33 GE-function parameters are estimated (plus unknown satellite/receiver differential delays). The satellite/receiver differential delay values are

constrained to 0.5 nanoseconds with respect to the values obtained from the nighttime fit (see Section 3.4).

3.4 Differential Delay Estimation Procedure

For each day, i.e. in 24-hour intervals, satellite/receiver differential delay values are determined in a special fit into which only global nighttime TEC data enter. A degree $n = 4$ and order $m = 2$ spherical harmonic is used to model the nighttime VTEC. The coefficients a_{10} , a_{11} and b_{11} , which define the origin of the coordinate reference, are kept fixed with zero. No a priori constraints are applied to the satellite/receiver differential delay values, no elevation-dependent weights are applied to the TEC observables. The satellite/receiver differential delays obtained from this nighttime fit are then introduced as reference values into all the other fits for that a day and are constrained with 0.5 nanoseconds in these solutions (see the above Sections 3.1 to 3.3).

4 COMPARISONS - RESULTS

Several Analysis Centers contributed ionospheric products for comparison over the GPSweeks 0823 to 0827: COD provided for these five weeks daily global VTEC maps in a $2^{\circ}.5$ grid. DLR and UNB delivered for weeks 0823 to 0825 hourly regional VTEC maps for the european area in 1° grids and daily satellite/receiver differential delay values. ESOC provided for all five weeks global 12-hour VTEC maps in a $2^{\circ}.5$ grid and 1° gridded local VTEC maps around the ESA ground sites Kiruna, Kourou, Madrid (instead of Villafranca), Maspalomas and Perth. ESOC's algorithms were described in the above Chapter 3. The mathematical approaches of COD, DLR and UNB can be found in (Schaer et al., 1995), (Engler et al., 1993), (Engler et al., 1995) and (Komjathy et al., 1996). Further methods of VTEC map computation are described in (Mannucci et al., 1993) and (Gao et al., 1994).

4.1 VTEC Maps

Five weeks of VTEC maps from four Analysis Centers are quite a lot amount of data to be compared and analyzed. To do this task efficiently, a certain scheme had to be worked out on how to make this intercomparison. The global VTEC maps of COD and ESOC were compared in 12-hour intervals. Comparison of - and with the regional VTEC maps of DLR and UNB and the local maps of ESOC was done in 6-hour intervals, i.e only the 0^h , 6^h , 12^h and 18^h maps of DLR and UNB were included into the comparison.

In the case that global $2^{\circ}.5$ grid maps were compared with 1° grid regional and local maps, linear interpolation was used to calculate VTEC values from the global $2^{\circ}.5$ grids in 1° intervals in the case of non-identical points.

Since the VTEC maps originating from the different Analysis Centers were referred to different reference epochs, rotations had to be made before the comparisons.

Concerning the local ESOC VTEC maps, only the results of the comparison with the Madrid maps were included in this paper.

In spite this comparison scheme reduced the number of possible combinations considerably, the remaining amount of VTEC map pairs to be compared was still too large to analyze all these comparisons by the inspection of plots. Additionally some statistics were appreciated. So a small program called "vteccm" was developed which performs a rapid comparison of two given VTEC maps and provides some general information on their agreement. To do this, vteccm calculates the differences between the two VTEC map files at all grid points. As already mentioned above, linear interpolation is used in non-identical grid points. Considering these differences as residuals, a residual VTEC map is obtained from which a mean offset between the two VTEC maps and a sigma with respect to this mean is calculated. In a next level the residual map is subdivided into 4 equally sized sub-parts, and for each part a sigma with respect to the overall mean is calculated. In the 3rd level the residual VTEC map is subdivided in 16 equally sized parts and the sigmas are computed, and so on. vteccm finally outputs:

- . The minimum and the maximum residual obtained.
- . The mean offset.
- . The overall sigma at the 1st level.
- . 4 sigmas at the 2nd level.
- . 16 sigmas at the 3rd level.
- and so on.

The sigmas at the different levels are arranged in matrix form where their positions in the matrix correspond to the locations of their sub-parts in the residual VTEC map. So from analyzing the sigmas at the different levels one can directly see in which parts of the compared area the differences between the two VTEC maps are the largest. As an example Figure 4.1 presents a vteccm output. In the south-east the residuals are at largest.

AC1: aaa AC2: bbb

the area that was finally compared:

latmax = 70.0 latmin = 30.0

lonmin = -20.0 lonmax = 40.0

vtec1: min = 2.6 max = 11.5 (minimum and maximum value of 1st VTEC map)

vtec2: min = 2.1 max = 16.1 (minimum and maximum value of 2nd VTEC map)

rvtec: min = -4.6 max = 5.2 (minimum and maximum value of the residual VTEC map)

xvtec: min = 2.6 max = 11.5 (minimum and maximum value of the interpolated VTEC map)

*** mean offset -0.26

sigmas at level 1

latitude/longitude range considered at level 1: latmax = 70.0 latmin = 30.0

lonmin = -20.0 lonmax = 40.0

0.145D+01

sigmas at level 2

latitude/longitude range considered at level 2: latmax = 70.0 latmin = 32.5
lonmin = -20.0 lonmax = 37.5

0.117D+01 0.513D+00
0.111D+01 0.180D+01

sigmas at level 3

latitude/longitude range considered at level 3: latmax = 70.0 latmin = 32.5
lonmin = -20.0 lonmax = 37.5

0.106D+01 0.112D+01 0.651D+00 0.148D+00
0.126D+01 0.130D+01 0.554D+00 0.580D+00
0.928D+00 0.810D+00 0.536D+00 0.147D+01
0.185D+01 0.420D+00 0.146D+01 0.298D+01

Figure 4.1: Example Output from the vteccm Program, all numbers are given in [TECU].

vteccm is invoked from a TCL for each VTEC map pair combination of one day, i.e. submission of this TCL once provided the vteccm comparison outputs of all VTEC map pair combinations for that day. The TCL was run for each day of the five weeks, and a quick look on maximum and minimum residuals, mean offset and 1st level sigma gave a fast overview. Only in critical cases - based on the vteccm output - closer consideration was done, i.e. in cases of large offsets and/or sigmas. Also a general overview over the day-to-day agreement of certain VTEC map pair combinations was easily obtained.

Figures 4.2 a-k show the comparison results for all considered VTEC map pair combinations, based on the vteccm output. Each plot contains 3 curves: The upper curve shows (mean offset + σ), the middle curve shows (mean offset), and the lower curve shows (mean offset - σ), i.e. at days at which all three curves are close together the agreement between two VTEC maps with respect to the mean offset is good, and in cases of big distances between the curves the agreement is bad.

The following Sub-sections 4.1.1 to 4.1.7 summarize the results obtained for the different comparisons according to the defined scheme, together with some remarks.

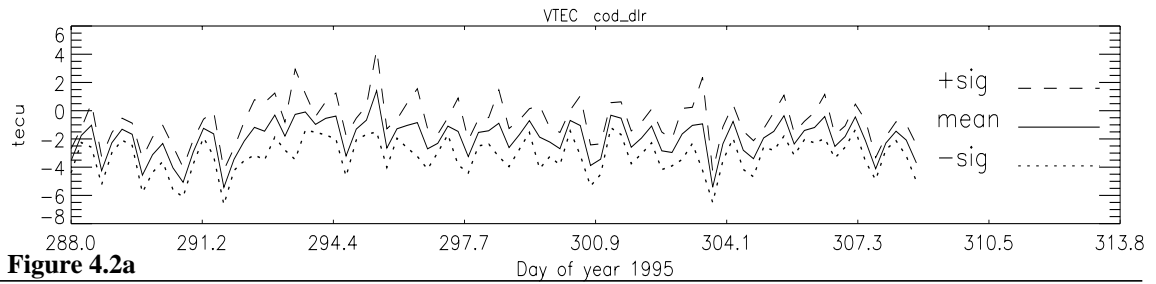


Figure 4.2a

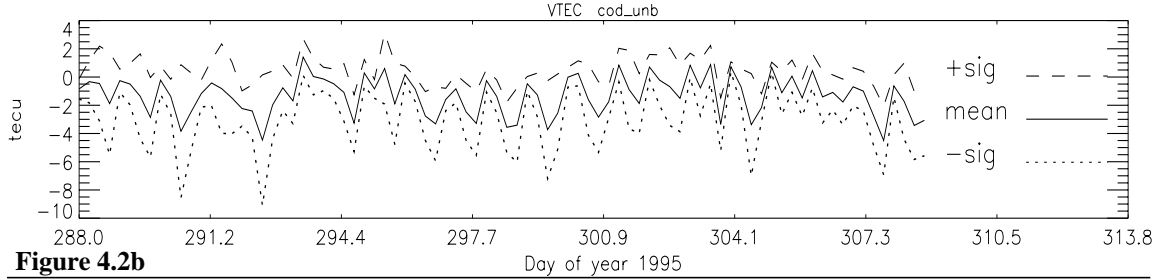


Figure 4.2b

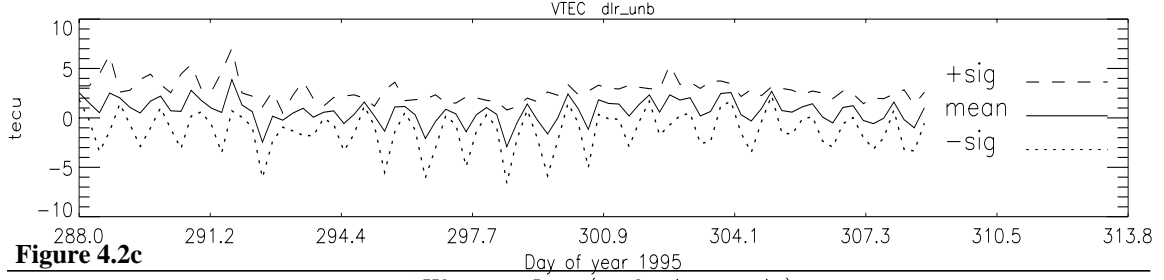


Figure 4.2c

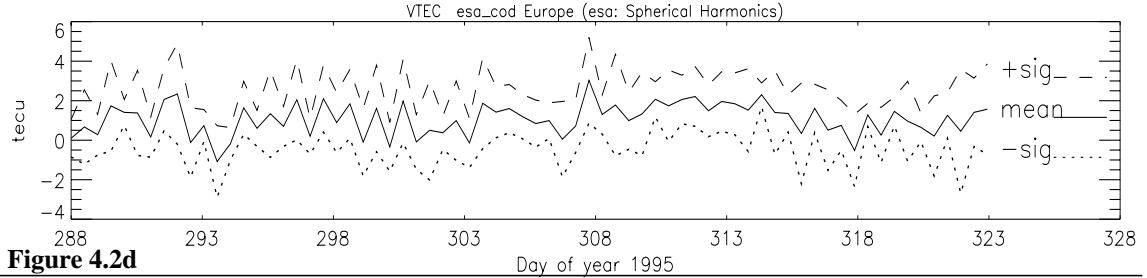


Figure 4.2d

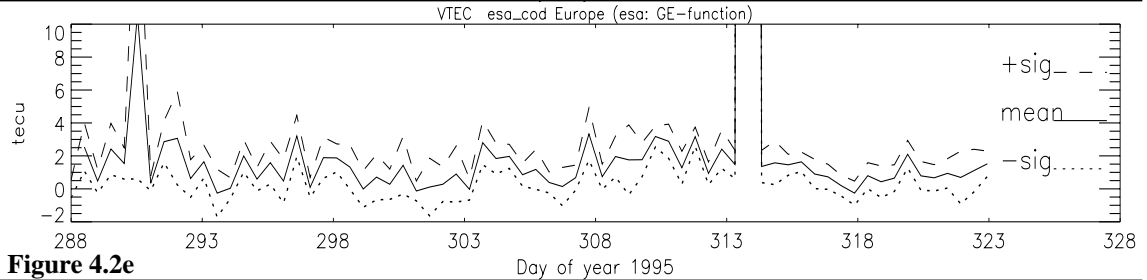


Figure 4.2e

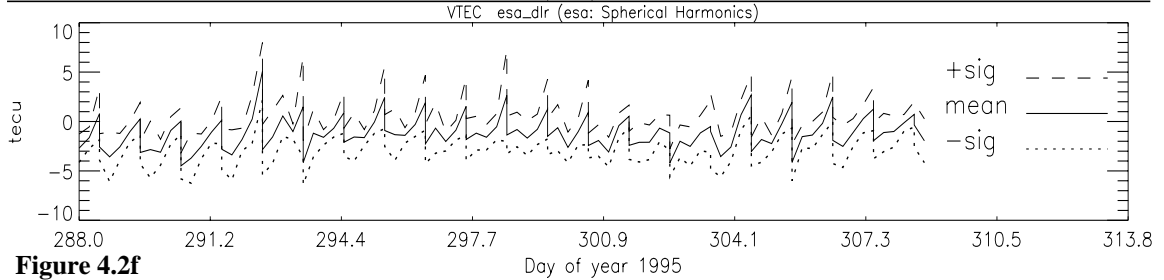
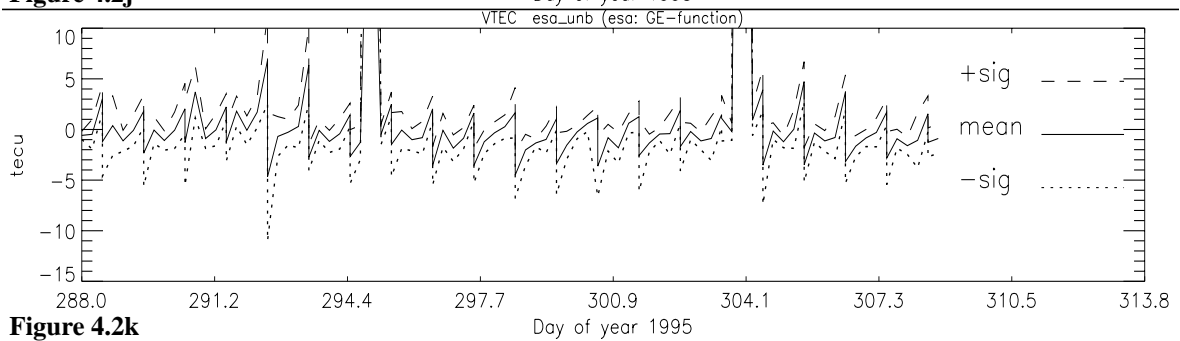
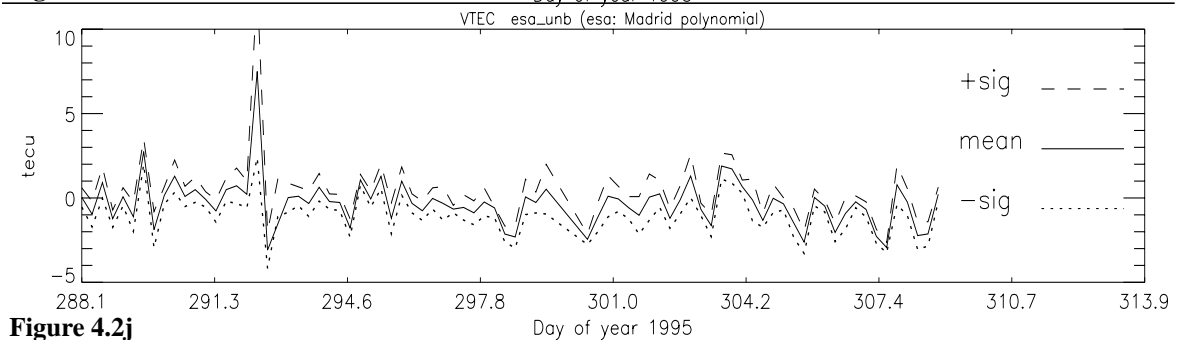
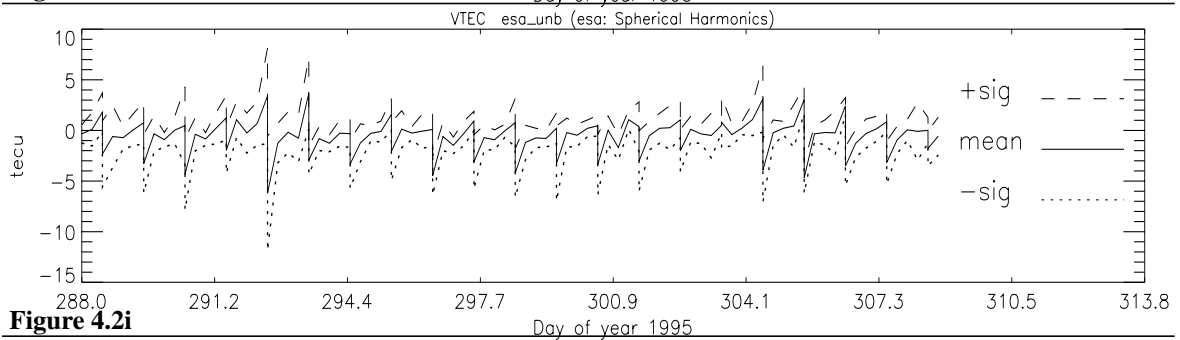
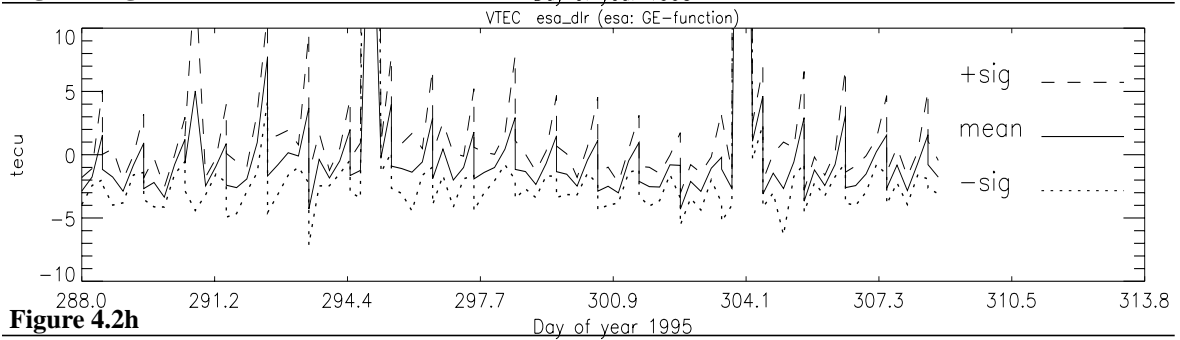
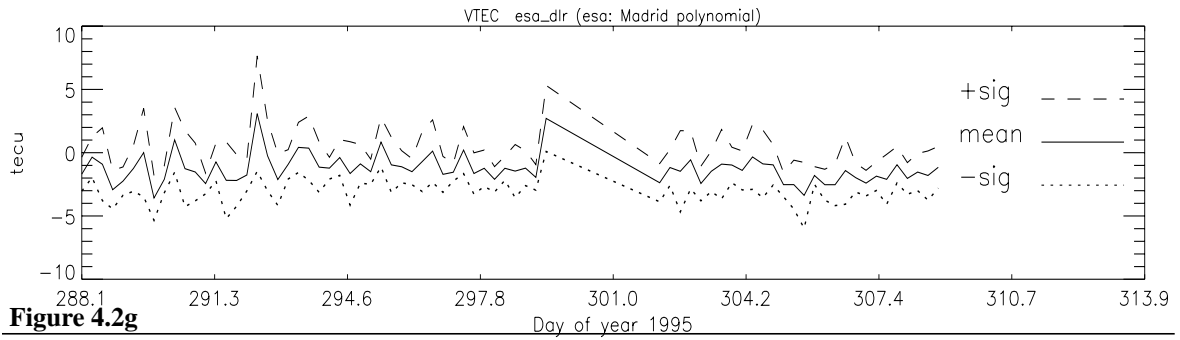


Figure 4.2f

Figures 4.2 a-f: Results of VTEC Map Comparison.



Figures 4.2 g-k: Results of VTEC Map Comparison.

4.1.1 Comparison COD \Leftrightarrow DLR

An offset of 1-5 TECU, in the mean about 2 TECU, can be observed between the COD and the DLR VTEC maps. The offset is always negative. That means that the COD maps are systematically lying below the DLR maps. The sigmas with respect to the daily offsets vary between 1 to 1.5 TECU. A closer look to some days with larger offsets and sigmas showed that generally the agreement seems to be better in the middle of the compared area than at the borders. Figure 4.2a shows the variation of the mean offset and the sigmas over the weeks 0823 - 0825.

4.1.2 Comparison COD \Leftrightarrow UNB

Again an overall negative offset can be recognized, in the mean about -1.5 TECU, i.e. the COD VTEC maps are again lying systematically below the foreign maps - in this case the UNB ones. With respect to the daily mean offsets sigmas of 1-3 TECU can be seen. A closer look to some days with larger offsets and sigmas showed that generally the agreement seems to be best in the center and in the north-east corner of the compared area. Figure 4.2b shows the variation of the mean offset and the sigmas over the weeks 0823 - 0825.

4.1.3 Comparison DLR \Leftrightarrow UNB

No significant systematic offset can be observed between the DLR and the UNB VTEC maps. The daily offsets seem to vary around 1-3 TECU, and the sigmas are in the same order. A closer look to some days with larger offsets and sigmas showed that generally the agreement seems to be worst in the south-east corner of the compared area. Figure 4.2c shows the variation of the mean offset and the sigmas over the weeks 0823 - 0825.

4.1.4 Comparison ESOC \Leftrightarrow COD

Only the global ESOC spherical harmonic and GE-function models were compared with the COD VTEC maps.

Comparison with ESOC spherical harmonics: Comparison was done globally and restricted to the european area. Since especially on the southern hemisphere there are large gaps in station coverage (ESOC uses only Rogue stations in its processing), the spherical harmonics are bad determined in these zones. This leads to abnormal spherical harmonic behaviour in these areas, which can be seen in the VTEC plots in form of high hills and holes of same depth directly near the hills. As the global comparison with COD showed, the mean offsets between ESOC and COD VTEC maps are quite small - but the sigmas are large, up to 10 TEC, and up to 80 TECU in areas where no observation data had entered into the ESOC processing.

So only the comparison results over the region of Europe are presented here. In the european area an overall offset of about 1 TECU can be recognized between ESOC and COD VTEC maps. This offset is always positive, but since COD were now subtracted from the other Analysis Center's maps - in this case ESOC, this means that COD lies again below the foreign model. With respect to this overall offset daily offsets and sigmas seem to vary around 1-2 TECU each. A closer look to some days with larger offsets and sigmas showed that there seems to be a trend that in the north-west corner of the compared area the agreement is worst. Figure 4.2d shows the variation of the mean offset and the sigmas over the weeks 0823 - 0827.

Comparison with GE-functions: Concerning station coverage, the GE-functions are affected similarly as the spherical harmonics, i.e. in areas with good station coverage the GE-functions are good too. Additionally GE-functions seem to be more vulnerable to bad receiver data. The Maspalomas station data, which was known to be problematic at that time, caused for instance every day an abnormal GE-function peak at high northern latitudes. Also the data of Kourou and the Seychelles was problematic. Further tests made as consequence of the comparison results have shown that, after these stations were excluded from GE-function processing, the high-latitude anomaly had disappeared or was at least drastically reduced. Also variations in the degree and order of GE-function development (e.g. $2n = 8, 2m = 4$; $2n = 10, 2m = 4$; $2n = 10, 2m = 8$) caused the anomaly to disappear. Further tests will be necessary to find out an optimal way of GE-function processing.

Because of the problems pointed out above, only the comparison results of the GE-function maps with the COD models over the region of Europe are presented here. As with the spherical harmonics, an overall offset of about 1 TECU can be recognized. Again this overall offset is positive, which means that the COD maps seem to lie below the GE-function models. With respect to this overall offset, daily offset variations of 1-2 TECU can be seen and sigmas around 1 TECU. On doy 290 and 313 large outliers are present. These outliers were caused by the above mentioned problematic stations. Apart from these outliers the GE-functions seem to be a little bit closer to the COD models as the ESOC spherical harmonics. A closer look to some days with larger offsets and sigmas seem to indicate that the agreement is a little bit worse in the southern and sometimes in the western part of the compared area. Figure 4.2e shows the variation of the mean offset and the sigmas over the weeks 0823 - 0827.

4.1.5 Comparison ESOC \Leftrightarrow DLR

Comparison with ESOC spherical harmonics: Because the ESOC spherical harmonics are well feeded with observation data in the european area (see above Section 4.1.4), the agreement with the DLR VTEC models is quite good. An overall mean offset of about -1 to -2 TECU seems to be present, which means that the ESOC models lie systematically below the DLR models. Around that overall offset variations and sigmas of about 3 TECU can be seen. Since the 12^h DLR models were compared with the 6^h and the 18^h ESOC spherical harmonic models (both rotated to 12^h), peaks appear every day at 12^h. A closer look to some days with larger offsets and sigmas showed that the worst agreement seems to be at the southern border of the compared area. Figure 4.2f shows the variation of the mean offset and the sigmas over the weeks 0823 - 0825.

Comparison with ESOC local polynomials for Madrid: Also the Madrid local polynomial models seem to show an overall offset of about 1 TECU below the DLR maps and around that overall offset variations and sigmas about 1-3 TECU. Around doy 300 there was a data gap. A closer look to some days with larger offsets and sigmas showed that the worst agreement seems to be in the north-west and sometimes in the south-east corner of the compared area. Figure 4.2g shows the variation of the mean offset and the sigmas over the weeks 0823 - 0825.

Comparison with GE-functions: As was pointed out in the above Section 4.1.4, the GE-functions had problems in the high northern latitudes. However, the european area, in which the GE-functions were compared with the DLR VTEC maps, is far enough in the south, so that the agreement was in most cases good. Only on some days, especially on doys 295 and 304, the high latitude anomaly propagated so far southward, that it was felt in the comparison. Except from these outliers, mean offsets up to 3 TECU are present without an overall offset. The sigmas around the mean offsets range between 1-3 TECU. Again the 12^h DLR maps were compared with the 6^h and the 18^h ESOC models (both rotated to 12^h). A closer look to some days with larger offsets and sigmas showed the worst

agreement in the north (for the reasons stated above) and sometimes in the south-east. Figure 4.2h shows the variation of the mean offset and the sigmas over the weeks 0823 - 0825.

4.1.6 Comparison ESOC \Leftrightarrow UNB

Comparison with ESOC spherical harmonics: As with the DLR models, the agreement with UNB over the european area is good. An overall offset of -1 TECU seems to be present, i.e. the ESOC maps are lying below the UNB maps. Around that overall offset the daily mean offsets and sigmas seem to vary about 2 TECU. From doy 294 on the variations become smaller but increase again at doy 304. Since the 12^h UNB models were compared with the 6^h and the 18^h ESOC spherical harmonic models (both rotated to 12^h), peaks appear every day at 12^h. A closer look to some days with larger offsets and sigmas showed the worst agreement to be in the north-west and in the south-east corner of the compared area. Figure 4.2i shows the variation of the mean offset and the sigmas over the weeks 0823 - 0825.

Comparison with ESOC local polynomials for Madrid: Madrid local polynomial models and UNB VTEC maps show very close agreement of 0-1 TECU in the daily mean offsets as well as in the sigmas. Only on doy 292 there is a significant outlier; on this day a large geomagnetic field disturbance occurred. A closer look to some days with larger offsets and sigmas showed the worst agreement to be in the north-west and in the south-east corner of the compared area. This north-west/south-east effect was also present in the 9-hour comparison for doy 292, together with a whole sigma level higher as usual. Figure 4.2j shows the variation of the mean offset and the sigmas over the weeks 0823 - 0825.

Comparison with GE-functions: Generally the agreement between GE-functions and UNB VTEC maps is about 1-3 TECU in the mean offsets and sigmas of 1 TECU around these offsets. Because of the problems stated in the above Section 4.1.4, the GE-functions showed sometimes abnormal behaviour in the high northern latitudes. Here this can be seen in form of outliers, especially on doys 295 and 304. Again the 12^h UNB maps were compared with the 6^h and the 18^h ESOC models (both rotated to 12^h). A closer look to some days with larger offsets and sigmas showed, that, apart from casual discrepancies in the north, worst agreement was found in the south-east part of the compared area. Figure 4.2k shows the variation of the mean offset and the sigmas over the weeks 0823 - 0825.

4.1.7 Comparison of ESOC Local with Global Models

As a representative of the five ESA ground sites for which local polynomial models were fitted to ESOC, only the results for Madrid were presented in the previous sections. To the agreement of the polynomial maps for Kiruna, Kourou, Maspalomas and Perth with the ESOC spherical harmonic and GE-function models some short remarks only:

- Generally good agreement was observed with the Kiruna, Madrid and Perth polynomials: 0-3 TECU mean offsets (1-6 TECU offsets at Perth with the spherical harmonics) and sigmas of 1-3 TECU with respect to these offsets.
- In the case of Kourou and Maspalomas the agreement was significantly worse. Especially from Maspalomas it is well known, that there were considerable receiver problems at the time for which the intercomparison was done. In particular during the week 0826 the Maspalomas data was bad, and in week 0827 Maspalomas provided tracking data only for one and a half day. Quite often unrealistic polynomials were obtained for both stations, Kourou and Maspalomas.
- Generally the GE-functions seem to be closer to the polynomial models than the spherical harmonics.

4.2 Differential Delays

Comparison of differential delays was done between results provided by DLR, UNB and ESOC. The UNB differential delay files contain differential delay values for all satellites and 6 ground stations. DLR provided values for all satellites, except PRN12 and PRN28, and for 16 ground stations. And ESOC determined values for all satellites and 64 ground stations.

The day-to-day variation in the values of all 3 series is in most cases within the 0.5 nanosecond limit. Especially the DLR and ESOC differential delay series seem to indicate a generally higher day-to-day scatter for the stations than for the satellites. Typical examples are Arequipa and Fortaleza. - There are of course also a lot of stations which show the same lower order of scatter as the satellites. The ESOC differential delay files show additionally a clear increase of sigmas of the mean values by a factor 2-3 for GPSweeks 0824 - 0827 with respect to week 0823. This can especially be seen at the satellites.

A comparison between the three series seem to indicate an offset of the DLR series of about 1 nanosecond with respect to the ESOC series, and the UNB series seems to be close to the ESOC results. This was also confirmed by A. Komjathy (private communication). ESOC uses 350 km as ionospheric shell height while DLR and UNB are using 400 km. So ESOC repeated the differential delay estimation for week 0823 also with 400 km shell height. However, no variances of more than 0.2 nanoseconds with respect to the 350 km solution for that week could be observed. A. Komjathy and R.B. Langley (1996) made similar calculations with the same result. Obviously the difference in shell height cannot explain this 1 nanosecond offset. The reason for this offset might come from differences in the algorithms used and/or from the different sets of ground stations used. Additionally DLR rejects the satellites PRN12 and PRN28 in its solution. Figure 4.3 compares the DLR, UNB and ESOC series exemplarily for 2 stations and 4 satellites.

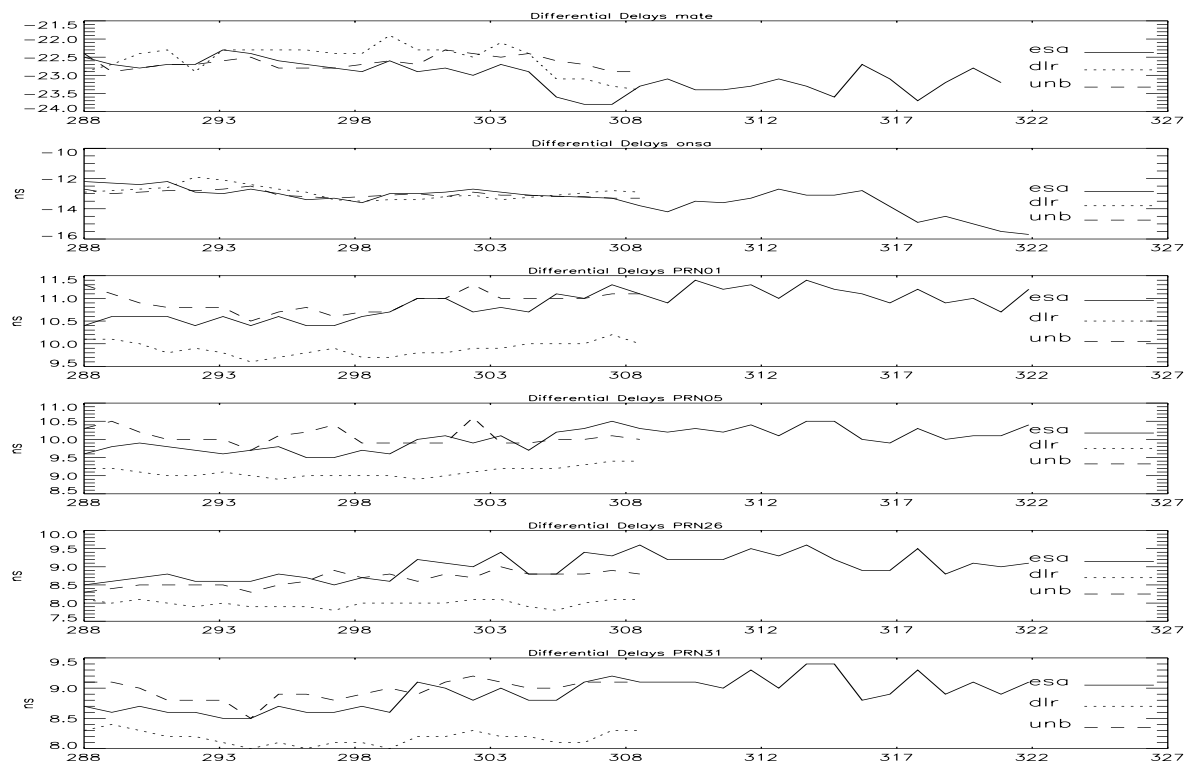


Figure 4.3: Differential Delay Behaviour for a selected Set of Stations and Satellites.

5 CONCLUSIONS

With regard to include ionosphere data into the IGS product list, an intercomparison of ionosphere products provided by different Analysis Centers was organized in preparation of the IGS workshop in Silver Spring in March 1996. Four Analysis Centers contributed to this comparison with own results.

In areas with tracking data of sufficient density the different VTEC models seem to show a general agreement of 5 TECU and better, normally about 3 TECU. For the differential delay values agreement within 1 nanosecond was achieved. In summary the intercomparison results look encouraging to do further steps into the direction of a routine provision of ionosphere maps as new part of IGS.

ESOC used the comparison as opportunity to verify its own mathematical modeling. The following weak points were identified from the analysis of the intercomparison results:

- The ground station net used by ESOC must be densified around the equator and at the southern hemisphere - gaps in station coverage have caused abnormal behaviour of global fits in weakly observed areas.
- Bad receiver data must be identified in a preprocessing step, since it had seriously affected the solutions.
- More testing is necessary to overcome the above mentioned problems and to achieve robust modeling.

Based on the knowledge earned from the intercomparison, the next steps into the direction of IGS must be undertaken now - relevant aspects are pointed out in ref. R4.

Beyond its IGS activities ESOC is also interested to use GPS-derived ionosphere maps to correct ERS-2 and other ESA satellite data.

Acknowledgments

The authors wish to express their acknowledgments to the Analysis Centers for their readiness to contribute to the intercomparison with own results and fruitful discussions. Thanks also to A. Komjathy and R.B. Langley for setting up the GPS-IONO mailing list at the University of New Brunswick which was very helpful for fast exchange of information and discussion.

6 REFERENCES

- R1. Biel, H.A. von (1990): 'The geomagnetic time and position of a terrestrial station.' Journal of Atmospheric and Terrestrial Physics, Vol. 52, No. 9, pages 687 - 694, 1990.
- R2. Engler, E., N. Jakowski, A. Jungstand and D. Klähn (1993): 'First experiences in TEC monitoring and modelling at the DLR Remote Sensing Station Neustrelitz.' Proceedings of the

- GPS/Ionosphere Workshop Modelling the Ionosphere for GPS Applications, DLR/DFD, Fernerkundungsstation Neustrelitz, Germany, September 29-30, 1993, pages 122-125.
- R3. Engler, E., E. Sardón and D. Klähn (1995): 'Real Time Estimation of Ionospheric Delays'. Proceedings of the ION GPS-95, 8th International Technical Meeting of The Satellite Division of The Institute of Navigation, Palm Springs, California, U.S.A., September 12-15, 1995.
- R4. Feltens, J. (1996): 'Ionosphere Models - A New Product of IGS ?', IGS Position Paper, Proceedings of the IGS Analysis Center Workshop, Silver Spring, MD, U.S.A., March 19-21, 1996.
- R5. Feltens, J. (1995a): 'GPS TDAF Ionosphere Monitoring Facility, Mathematical Model Developments'. GTDAF-TN-08 Iss 1/- 11 Sep-95 (ESOC-internal document).
- R6. Feltens, J. (1995b): 'GPS TDAF Ionosphere Monitoring Facility, Examination of the Applicability of Gauss-Type Exponential Functions to Ionospheric Modeling'. GTDAF-TN-09 Iss 1/- 11 Sep-95 (ESOC-internal document).
- R7. Gao, Y., P. Heroux and J. Kouba (1994): 'Estimation of GPS Receiver and Satellite L1/L2 Signal Delay Biases Using Data from CACS'. Proceedings of the International Symposium on Kinematic Systems in Geodesy (KIS94), Geomatics and Navigation, Banff, Canada, August 30 - September 2, 1994, pages 109-117.
- R8. Komjathy, A. and R.B. Langley (1996): 'An Assessment of Predicted and Measured Ionospheric Total Electron Content Using a Regional GPS Network'. Proceedings of the ION GPS-96, 9th International Technical Meeting of The Satellite Division of The Institute of Navigation, Santa Monica, California, U.S.A., January 22-24, 1996.
- R9. Mannucci, A.J., B.D. Wilson and C.D. Edwards (1993): 'A New Method for Monitoring the Earth's Ionospheric Total Electron Content Using the GPS Global Network'. Proceedings of the ION GPS-93, 6th International Technical Meeting of The Satellite Division of The Institute of Navigation, Salt Lake City, Utah, U.S.A., September 22-24, 1993, Vol. II, pages 1323-1332.
- R10. Newby, S.P. (1992): 'An Assessment of Empirical Models for the Prediction of the Transionospheric Propagation Delay of Radio Signals'. University of New Brunswick, Dept. of Surveying and Engineering, Canada, Technical Report No. 160, August 1992.
- R11. Schaer, S., G. Beutler, L. Mervart, M. Rothacher and U. Wild (1995): 'Global and Regional Ionosphere Models Using the GPS Double Difference Phase Observable'. Paper presented at the 1995 IGS Workshop, Potsdam, Germany, May 15-17, 1995.